Recent Northern Hemisphere snow cover extent trends and implications for the snow-albedo feedback

Stephen J. Déry[1*] and Ross D. Brown[2]

[1]Environmental Science and Engineering Program, University of Northern British Columbia, Prince George, BC, V2N 4Z9, Canada

[2]Section des processus climatiques, Environnement Canada à Ouranos, Montréal, QC, H3A 1B9, Canada

[*]To whom correspondence should be addressed; E-mail: sdery@unbc.ca

October 5, 2007

Monotonic trend analysis of Northern Hemisphere snow cover extent (SCE) over the period 1972-2006 with the Mann-Kendall test reveals significant declines in SCE during spring over North America and Eurasia, with lesser declines during winter and some increases in fall SCE. The weekly mean trend attains $-$1.28, $-$0.78, and $-$0.48 $\times$ 10^6 km^2 (35 years)$^{-1}$ over the Northern Hemisphere, North America, and Eurasia, respectively. The standardized SCE time series vary and trend coherently over Eurasia and North America, with evidence of a poleward amplification of decreasing SCE trends during spring. Multiple linear regression analyses reveal a significant dependence of the retreat of the spring continental SCE on latitude and elevation. The poleward amplification is consistent with an enhanced snow-albedo feedback over

northern latitudes that acts to reinforce an initial anomaly in the cryospheric system.

1. Introduction

Snow cover over the Northern Hemisphere (NH) ranges, on average, from a minimum extent of 2 $\times 10^6$ km^2 each August to a maximum extent of 45 $\times 10^6$ km^2 each January or nearly one half of the NH land surface [*Lemke et al.*, 2007]. Because of its large seasonal variability and distinctive physical properties, snow plays a major role in the climate system through strong positive feedbacks related to albedo [e.g., *Groisman et al.*, 1994a] and other weaker feedbacks related to moisture storage, latent heat, and insulation of the underlying surface [*Stieglitz et al.*, 2003]. The snow-albedo feedback, along with the ice-albedo feedback, is invoked as a leading cause of amplified warming in polar and mountainous regions [*Serreze and Francis*, 2006; *Fyfe and Flato*, 1999]. Consistent with this hypothesis, changes in snow cover duration during the first and second halves of the hydrological year over 1967-2004 show a contrasting seasonal response, with the largest decreases occurring in spring over mainly NH high elevations [*Robinson and Dewey*, 1990; *Groisman et al.*, 1994a; *Fyfe and Flato*, 1999].

The main objective of this study is to investigate the spatial and temporal characteristics of recent trends in NH snow cover in more detail to provide an improved understanding of current changes. This is carried out through analysis of weekly trends in NH, North American and Eurasian SCE for the period 1972-2006. Trends are analyzed at a weekly scale to maximize the temporal resolution of the dataset. This is important as changes may not be apparent when analyzed at the more conventional monthly scale. The implications of recent trends in weekly SCE on the snow-albedo feedback are also assessed to explore its possible influence on global climate change.

2. Data and Methods

Weekly values of SCE from January 1972 to December 2006 are extracted from the National Oceanic and Atmospheric Administration (NOAA) weekly SCE dataset [*Robinson et al.*, 1993] maintained at Rutgers University (http://climate.rutgers.edu/snowcover/). The satellite-based data provide weekly SCE for the land masses of Eurasia, North America and the NH as a whole. Greenland is excluded from the analyses as its snow cover (as seen by the predominantly visible satellite systems used in the NOAA product) is mainly perennial in nature. The study is restricted to the post-1971 period as there are some missing charts in the 1967-1971 data reanalyzed by *Robinson* [2000]. The weekly snow cover analysis procedure changed in May 1999 with the introduction of the daily Interactive Multi-Sensor (IMS) snow cover product [*Ramsay*, 1998] at a much higher resolution (≈25 km) than the 190.5 km weekly product. To maintain continuity a pseudo-weekly product is derived from IMS by taking each Sunday map as representative of the previous week. This has resulted in obvious inconsistencies at some gridpoints which are screened out of this analysis. *Brown et al.* [2007] are unable to find any strong evidence of inhomogeneities in the NOAA SCE series over northern Canada before and after 1999 but a recent analysis by D. A. Robinson (personal communication, 2007) shows that the pre-1999 charts overestimate snow cover in mountainous regions during the spring-summer ablation period.

The NOAA dataset is considered reliable for continental-scale studies of snow cover variability [*Wiesnet et al.*, 1987] but it has received only limited validation over higher latitudes and mountainous regions. Recent evaluations of the NOAA dataset over northern Canada [*Wang et al.*, 2005; *Brown et al.*, 2007] show it overestimates snow cover during spring and summer and becomes decoupled from air temperature anomalies in July. These results along with the recent findings of Robinson suggest that the summer (July, August) SCE series may not be suitable for trend analysis. They are included in this paper to maintain continuity in the plots but are shaded to indicate their larger level of uncertainty.

Statistically significant ($p < 0.05$) monotonic trends in weekly SCE are assessed with the non-parametric Mann-Kendall test [*Mann*, 1945; *Kendall*, 1975; *Déry et al.*, 2005a]. The analysis is performed on the raw data as well as standardized series of weekly SCE based on a 1972-2006 reference period for computing the mean and standard deviation. Monotonic trends are expressed in terms of four quantities: absolute values in SCE ($\times 10^6$ km^2), as a percentage change from their initial values based on the associated Kendall-Theil Robust Lines [*Theil*, 1950; *Déry et al.*, 2005a], in standardized units over the study period, and finally, in terms of insolation-weighted anomalies. The latter are included in the analyses to explore the potential influence of the snow-albedo feedback on the observed SCE trends. The insolation-weighted anomalies are computed by multiplying the absolute values of SCE by the ratio of the weekly average and annual maximum incoming solar radiation at 60°N [*Pielke et al.*, 2000]. Thus the weights associated with the solar cycle vary sinusoidally with extreme values of unity at the summer solstice and of 0.05 at the winter solstice. The insolation-weighted values do not take into account cloud cover effects and the surface type underlying the snowpack and as such they represent the possible maximum influence of snow on the surface radiation budget.

Autocorrelation is known to affect trends in hydrometeorological variables such as river discharge that exhibit temporal persistence [*Yue et al.*, 2002; *Déry and Wood*, 2005]. Since SCE also exhibits persistence on monthly and annual timescales [e.g., *Déry et al.*, 2005b], we follow the methodology of *Yue et al.* [2002] to assess the influence of serial correlations on the trend analyses. Results based on the "pre-whitened" time series are therefore presented when year-to-year autocorrelations in SCE and their respective trends are statistically-significant.

3. Results

An important characteristic of continental snow covers is their tendency to exhibit persistent anomalies of a given sign. Analysis of the autocorrelation in the weekly standardized snow cover anomalies shows that series are significantly autocorrelated for periods of up to 16 weeks during spring in Eurasia and North America (Fig. 1a). The number of lagged weeks with statistically-significant autocorrelations diminishes approximately linearly during summer for all three regions of interest. This indicates that spring SCE anomalies impose a memory in the climate system that is not erased until the end of the summer when the SCE nears its minimum (19 August for the NH). Spring SCE also exhibits significant autocorrelations at an annual time scale, with year-to-year autocorrelations approaching 0.4 in the NH (Fig. 1b). Week-to-week autocorrelations with a one month time lag are nearly all statistically-significant during spring, with the highest values nearing 0.8 in June.

Strong negative trends in SCE are observed over the 35-year period in North America and Eurasia (Fig. 2a). Excluding July and August, statistically-significant trends in the absolute values of SCE are found from March to June for the NH, from April to June in North America, and in March as well as from late April to June in Eurasia. The largest decline in NH SCE occurs during the first week of June. The only statistically-significant positive trends are observed in Eurasia and the NH during November and December in response to a slight cooling over northern Eurasia during the 1972-2006 period.

Table 1 provides the 1972 to 2006 annual mean trend in weekly SCE for each region of interest, with and without the months of July and August. The mean trend in weekly SCE over the period 1972-2006 is greater for North America than Eurasia, both in absolute and relative terms. The positive trends in fall weekly SCE in Eurasia, features not observed in North America, partially offset the spring and summer declines in snow cover over this region. There are statistically-significant negative trends in weekly SCE over nearly half the year for the NH, and only two weeks showing statistically-significant, positive trends. Serial correlation affects about half of the statistically-significant trends.

Expressing the trends as relative departures from the initial values in 1972 according to the Kendall-Theil Robust Lines emphasizes the strong declines in SCE during spring and summer (Fig. 2b). The near disappearance of snow during summer over the 35-year period may be associated with data deficiencies (see Section 2).

Trends in standardized time series of SCE reveal surprisingly coherent responses over Eurasia and North America (Fig. 2c); the two trend series are significantly correlated with r = 0.83 (p <0.001). Trends during the first few months of the year are relatively weak but amplify during spring and summer, reaching declines as large as 2.0 standardized units in weekly NH SCE values by late June. The amplification exhibits a strong linear evolution with time from January to June with statistically-significant ($p < 0.001$), linear correlation coefficients of -0.92, -0.82 and -0.89 for NH, North America and Eurasia, respectively.

Insolation weighting of weekly trends to infer the snow-albedo feedback potential shifts the strongest trends toward the summer solstice when incoming solar radiation peaks in the NH (Fig. 2d). Late spring and early summer SCE trends thus have the greatest potential to directly affect the surface radiation budget whereas late fall positive SCE trends are suppressed.

Diagrams of standardized SCE anomalies (Fig. 3) reveal the shift toward negative anomalies after $\sim$1985 which corresponds with the ≈ 5% drop in annual mean NH SCE in the late 1980's noted by *Lemke et al.* [2007]. These plots also demonstrate the persistence of SCE anomalies onward from spring, with linear features showing horizontal (week to week) rather than vertical (year to year) structure. The contour plots for North America and Eurasia show considerable co-variability. In fact, the correlation coefficient between the two time series of weekly continental standardized SCE anomalies reaches r = 0.41 ($p < 0.001$). The standardized anomalies in SCE are of the same sign 64% of the time, further demonstrating the co-variability of the

North American and Eurasian snow covers. This number increases to 88% when simultaneous departures of at least one standard deviation of the same sign are considered, a feature observed on 250 occasions or 14% of the time over the period of record.

4. Concluding Discussion

Fig. 2c shows remarkable declines in standardized SCE anomalies with evidence of a poleward amplification in the strength of the trends from January to June. It is proposed that this amplification is attributable to the stronger albedo feedback over high latitudes that acts to reinforce an initial anomaly. Also, the transfer of temperature anomalies into components of the cryosphere with longer memory than snow cover (i.e. sea ice, sea surface temperature) will act to increase the persistence of an initial snow cover anomaly that started over mid-latitudes. In addition, the increasing land/ice cover fraction moving poleward may provide greater sensitivity to the snow-ice/albedo feedback. The persistence of SCE anomalies of a given sign and magnitude is particularly evident in the contour diagrams (Fig. 3).

The coherent variability and trends observed in North American and Eurasian SCE are consistent with the results of *Gutzler and Rosen* [1992] and others. The spatial coherence in the intercontinental snow covers and the temporal persistence on weekly and annual time scales are possible manifestations of the snow-albedo feedback. These features in the cryospheric system suggest that a hemispheric-scale mechanism is driving the SCE variability and trends. Surface air temperatures are anticorrelated to SCE anomalies [*Karl et al.*, 1993], implying that recent declines in SCE may be attributed in part to NH warming [e.g., *Stewart et al.*, 2005].

The insolation-weighted results provide some insights into the possible contribution of snow to the global surface radiation budget. The trend analyses show that the pronounced declines in continental snow cover during spring have a potentially much greater role in the surface radiation budget than the modest increases in fall SCE. Similarly, an analysis of “temperature sensitive regions” (TSRs) [*Groisman et al.*, 1994b] suggests greater sensitivity to SCE changes during spring than in other seasons (see auxiliary material for a description of the TSR analyses). The results indicate the greatest maximum snow-albedo feedback potential to the NH occurs in the April to June period with Eurasia exhibiting a greater feedback potential due to a larger TSR area than North America. These results are consistent with the insolation weighted SCE trends (Fig. 2d) and confirm the findings of *Groisman et al.* [1994a] that the land surface radiation budget, and hence the global climate system as a whole, may be most sensitive to changes in spring SCE.

Topography may also be playing a role in the observed decrease in spring snow cover through an enhanced snow-albedo feedback [*Fyfe and Flato*, 1999]. To investigate this further a multiple linear regression analysis is carried out of the trend in spring snow cover duration over 1972-2006 for each NOAA snow covered cell. Spring snow cover is defined as the number of days with snow cover in the February to July period and is analogous to the date of snow cover disappearance. The regression includes three variables: grid cell latitude, longitude and mean elevation. The analysis is done separately for North America and Eurasia owing to the different latitudinal distributions of snow cover on both continents.

These variables explain only a small fraction of the total variance (< 10%) as the spatial pattern of snow cover trends is strongly modulated by variability and change in regional temperature and precipitation. However, the analysis provides insights into the sign and importance of latitude and elevation over both continents. For North America, the analysis reveals that longitude (positive) and mean elevation (negative) are significant variables ($p < 0.05$), implying that the largest changes in spring snow cover are found over western parts of the continent and at higher elevations. For Eurasia, mean elevation (negative) and latitude (negative) are significant variables, indicating that spring snow decreases are larger at higher latitudes and elevations.

Note that these results are a function of the resolution of the NOAA dataset and that there are observations from high elevation regions showing recent increases in snowpack in response to increasing precipitation [e.g., *Zhang et al.*, 2004]. NOAA grid cells are $\approx$200 $\times$ 200 km and snow is only recorded when $\geq$ 50% of this area is snow covered. This spatial averaging likely implies the NOAA product detects snow cover changes in the lower elevations of mountains. Given the strong elevation dependence seen in snow cover trends in mountainous regions [e.g., *Mote*, 2006], it would be useful to quantify the elevation ranges the NOAA product monitors and to know whether this has changed in response to the increasing resolution of the daily snow maps used to derive the weekly products.

To summarize, strong negative trends in weekly SCE over the period 1972-2006 are observed in the NH, North America and Eurasia. The largest declines occur during spring over North America and, to a lesser extent, over Eurasia. Persistence both on weekly and annual times scales influences trends in North American and Eurasian SCE. The similar response of the North American and Eurasian snow covers, including their co-variability, persistence, and amplified trends during spring, provide evidence of the snow-albedo feedback as a possible mechanism driving these recent changes in observed SCE. Thus future work will address the interactions between atmospheric processes and topography (latitude, altitude, and underlying surface and vegetation types) to explain the mechanisms yielding spatial variability in SCE trends between North America and Eurasia. This will provide crucial information on the role of the snow-albedo feedback on the retreat of the continental snow cover and its possible influence on global climate change.

Acknowledgments

We thank D. A. Robinson and T. Estilow (Rutgers) for access to the SCE data and B. Ainslie (UNBC), A. Rennermalm (Princeton) and D. A. Robinson (Rutgers) for helpful comments on the paper. Supported by the Natural Sciences and Engineering Research Council and the Canada

Research Chair Program of the Government of Canada.

References

Brown, R. D., C. Derksen, and L. Wang (2007), Assessment of spring snow cover duration variability over northern Canada from satellite datasets, *Remote Sens. Environ.*, in press.

Déry, S. J., and E. F. Wood (2005), Decreasing river discharge in northern Canada, *Geophys. Res. Lett.*, *32*, L10401, doi: 10.1029/2005GL022845.

Déry, S. J., M. Stieglitz, E. C. McKenna, and E. F. Wood (2005a), Characteristics and trends of river discharge into Hudson, James, and Ungava Bays, 1964-2000, *J. Clim.*, *18*, 2540-2557.

Déry, S. J., J. Sheffield, and E. F. Wood (2005b), Connectivity between Eurasian snow cover extent and Canadian snow water equivalent and river discharge, *J. Geophys. Res.*, *110*, D23106, doi: 10.1029/2005JD006173.

Fyfe, J. C., and G. M. Flato (1999), Enhanced climate change and its detection over the Rocky Mountains, *J. Clim.*, *12*, 230-243.

Groisman, P. Ya., T. R. Karl, and R. W. Knight (1994a), Observed impact of snow cover on the heat balance and the rise of continental spring temperatures, *Science*, *263*, 198-200.

Groisman, P. Ya., T. R. Karl, R. W. Knight and G. L. Stenchikov (1994b), Changes of snow cover, temperature and radiative heat balance over the Northern Hemisphere, *J. Clim.*, *7*, 1633-1656.

Gutzler, D. S. and R. D. Rosen (1992), Interannual variability of wintertime snow cover across the Northern Hemisphere, *J. Clim.*, *5*, 1441-1447.

Karl, T. R., P. Y. Groisman, R. W. Knight, and R. R. Heim (1993), Recent variations of snow cover and snowfall in North America and their relation to precipitation and temperature variations, *J. Clim.*, *6*, 1327-1344.

Kendall, M. G. (1975), *Rank Correlation Methods*, 202 pp., Oxford Univ. Press, New York.

Lemke, P., et al. (2007), Observations: Changes in snow, ice and frozen ground, in *Climate Change 2007: The Physical Science Basis*, edited by S. Solomon et al., pp. 337-383, Cambridge

Univ. Press, London.

Mann, H. B. (1945), Non-parametric test against trend, *Econometrika*, *13*, 245-259.

Mote, P. W. (2006), Climate-driven variability and trends in mountain snowpack in Western North America, *J. Clim.*, *19*, 6209-6220.

Pielke, R. A. Sr., G. E. Liston, A. Robock (2000), Insolation-weighted assessment of Northern Hemisphere snow-cover and sea-ice variability, *Geophys. Res. Lett.*, *27*, 3061-3064.

Ramsay, B. (1998), The interactive multisensor snow and ice mapping system, *Hydrol. Processes*, *12*, 1537-1546.

Robinson, D. A. (2000), Weekly Northern Hemisphere snow maps: 1966-1999, *Preprints 12th Conference on Applied Climatology*, Asheville, NC, American Meteorol. Soc., 12-15.

Robinson, D. A. and K. F. Dewey (1990), Recent secular variations in the extent of Northern Hemisphere snow cover, *Geophys. Res. Lett.*, *17*, 1557-1560.

Robinson, D. A., K. F. Dewey, and R. R. Heim (1993), Global snow cover monitoring: An update, *Bull. Am. Meteorol. Soc.*, *74*, 1689-1696.

Serreze, M. C. and J. A. Francis (2006), The polar amplification debate, *Clim. Change*, *76*, 241-264.

Stewart, I. T., D. R. Cayan, and M. D. Dettinger (2005), Changes toward earlier streamflow timing in western North America, *J. Clim.*, *18*, 1136-1155.

Stieglitz, M., S. J. Déry, V. E. Romanovsky, and T. E. Osterkamp (2003), The role of snow cover in the warming of arctic permafrost, *Geophys. Res. Lett.*, *30*, 1721, doi: 10.1029/2003GL017337.

Theil, H. (1950), A rank-invariant method of linear and polynomial regression analysis, *Indagationes Math.*, *12*, 85-91.

Wang, L., M. Sharp, R. Brown, C. Derksen, and B. Rivard (2005), Evaluation of spring snow covered area depletion in the Canadian Arctic from NOAA snow charts, *Remote Sens. Environ.*, *95*, 453-463.

Wiesnet, D. R., C. F. Ropelewski, G. J. Kukla, and D. A. Robinson (1987), A discussion of the accuracy of NOAA satellite-derived global seasonal snow cover measurements, *Large Scale Effects of Seasonal Snow Cover*, edited by B. E. Goodison, R. G. Barry, and J. Dozier, IAHS Publ., *166*, 291-304.

Yue, S., P. Pilon, B. Phinney, and G. Cavadias (2002), The influence of autocorrelation on the ability to detect trend in hydrological series, *Hydrol. Processes*, *16*, 1807-1829.

Zhang, Y. S., T. Li, and B. Wang (2004), Decadal change of the spring snow depth over the Tibetan Plateau: The associated circulation and influence on the East Asian summer monsoon, *J. Clim.*, *17*, 2780-2793.

Table 1: Weekly mean and trend (based on the Mann-Kendall test) in SCE for the Northern Hemisphere (NH), North America (NA) and Eurasia, 1972-2006. The number of weeks with positive (SIG+), negative (SIG−), and serially uncorrelated (SU) statistically-significant ($p < 0.05$) trends in SCE for each region is also listed. Values in parentheses denote statistics computed excluding the months of July and August.

Statistic	NH	NA	Eurasia
Mean SCE ($\times 10^6$ km^2)	23.8 (28.9)	8.7 (10.5)	15.1 (18.5)
Mean Trend ($\times 10^6$ km^2 (35 years)$^{-1}$)	−1.28 (−0.96)	−0.78 (−0.61)	−0.48 (−0.35)
SIG+ (Weeks)	2 (2)	0 (0)	4 (4)
SIG− (Weeks)	24 (14)	23 (13)	20 (10)
SU (Weeks)	11 (10)	12 (11)	13 (12)

Figure Legends

Figure 1: a) Number of weeks or years with statistically-significant ($p < 0.05$) autocorrelations in the weekly standardized SCE anomalies for the Northern Hemisphere, North America, and Eurasia, 1972-2006. b) Year-to-year and c) week-to-week (lag of 4 weeks) autocorrelations in the weekly standardized SCE anomalies for the Northern Hemisphere, North America and Eurasia, 1972-2006. Dots indicate statistically-significant ($p < 0.05$) autocorrelations and the shading denotes the period with the largest level of data uncertainty.

Figure 2: Monotonic trends in weekly values of SCE for the Northern Hemisphere, North America, and Eurasia, 1972-2006. Trends are expressed in terms of a) the absolute values in SCE ($\times 10^6$ km^2), b) as a percentage change from their initial values based on the associated Kendall-Theil Robust Lines, c) in standardized units (s.u.) over the study period, and d) in terms of insolation-weighted anomalies. Dots in panels a) and c) denote statistically-significant ($p < 0.05$) trends and open circles mark statistically-significant trends affected by serial correlation. Dashed lines in c) represent linear regressions performed on the time series of trends in weekly standardized SCE anomalies from the first week of January to the last week of June. Shading denotes the period with the largest level of data uncertainty.

Figure 3: Contours of the weekly standardized SCE anomalies for the Northern Hemisphere, North America, and Eurasia, 1972-2006. The largest level of data uncertainty occurs from days 182 to 245 (July and August).

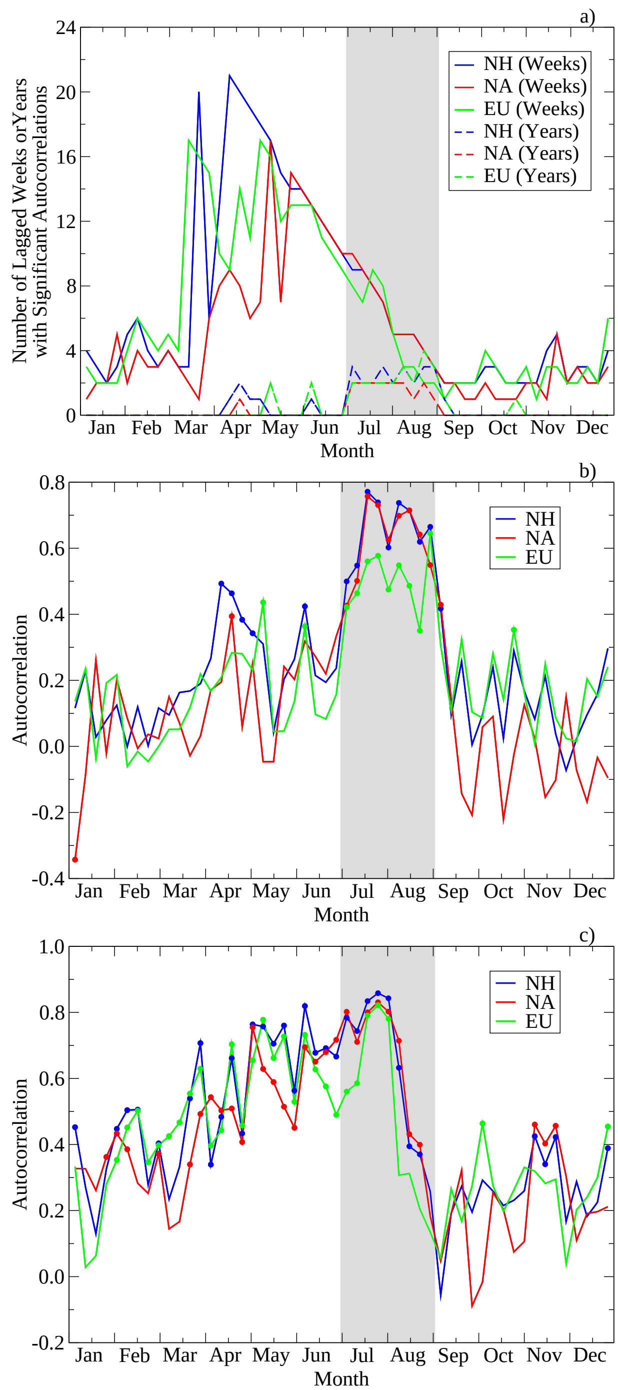
a)
Number of Lagged Weeks orYears with Significant Autocorrelations
NH (Weeks)
NA (Weeks)
EU (Weeks)
NH (Years)
NA (Years)
EU (Years)
Jan Feb Mar Apr May Jun Jul Aug Sep Oct Nov Dec
Month
b)
Autocorrelation
NH
NA
EU
Jan Feb Mar Apr May Jun Jul Aug Sep Oct Nov Dec
Month
c)
Autocorrelation
NH
NA
EU
Jan Feb Mar Apr May Jun Jul Aug Sep Oct Nov Dec
Month

Figure 1:

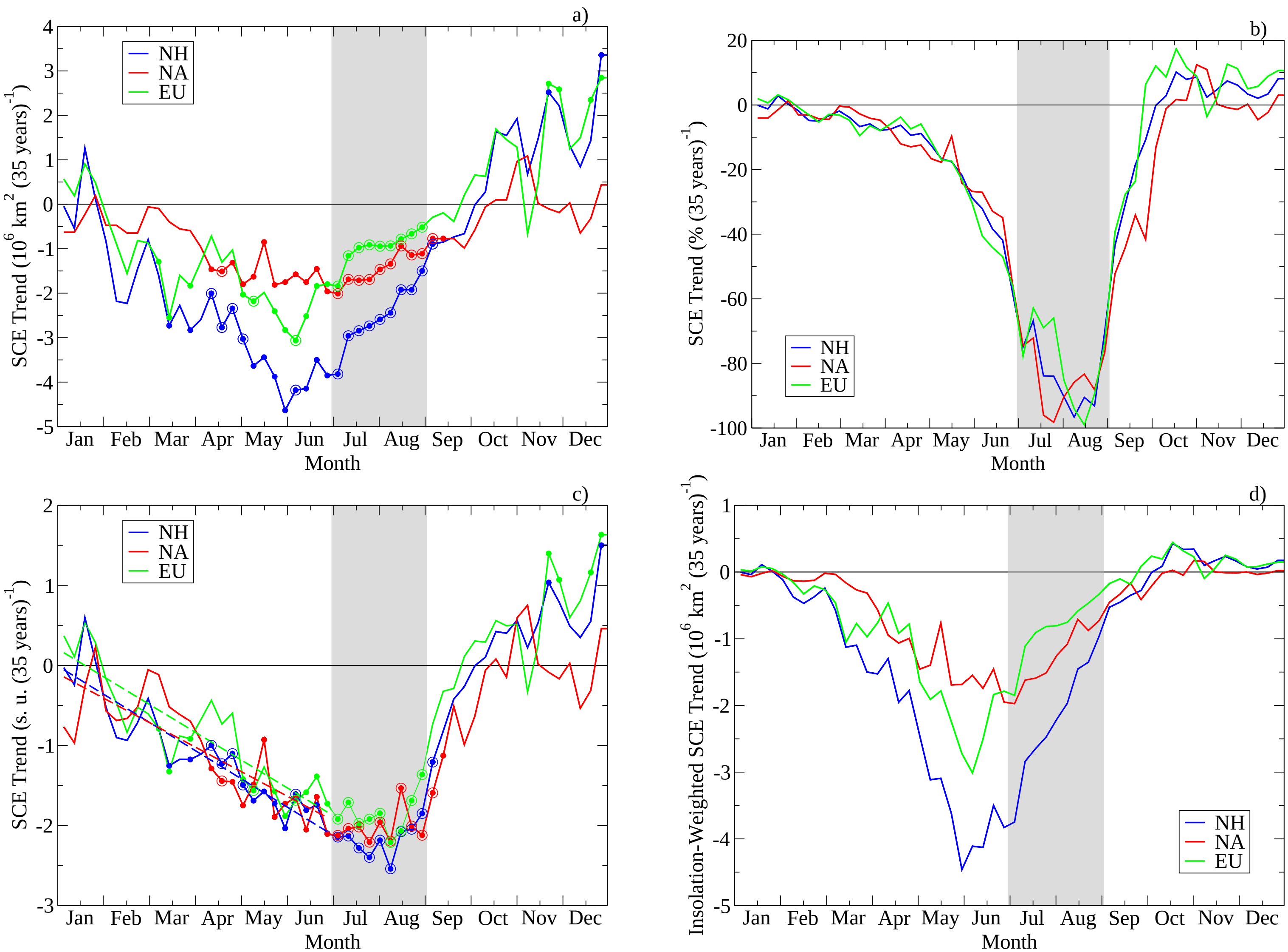
a)
NH
NA
EU
SCE Trend (10^6 km^2 (35 years)$^{-1}$)
4
3
2
1
0
-1
-2
-3
-4
-5
Jan Feb Mar Apr May Jun Jul Aug Sep Oct Nov Dec
Month
b)
NH
NA
EU
SCE Trend (% (35 years)$^{-1}$)
20
0
-20
-40
-60
-80
-100
Jan Feb Mar Apr May Jun Jul Aug Sep Oct Nov Dec
Month
c)
NH
NA
EU
SCE Trend (s. u. (35 years)$^{-1}$)
2
1
0
-1
-2
-3
Jan Feb Mar Apr May Jun Jul Aug Sep Oct Nov Dec
Month
d)
NH
NA
EU
Insolation-Weighted SCE Trend (10^6 km^2 (35 years)$^{-1}$)
1
0
-1
-2
-3
-4
-5
Jan Feb Mar Apr May Jun Jul Aug Sep Oct Nov Dec
Month

Figure 2:

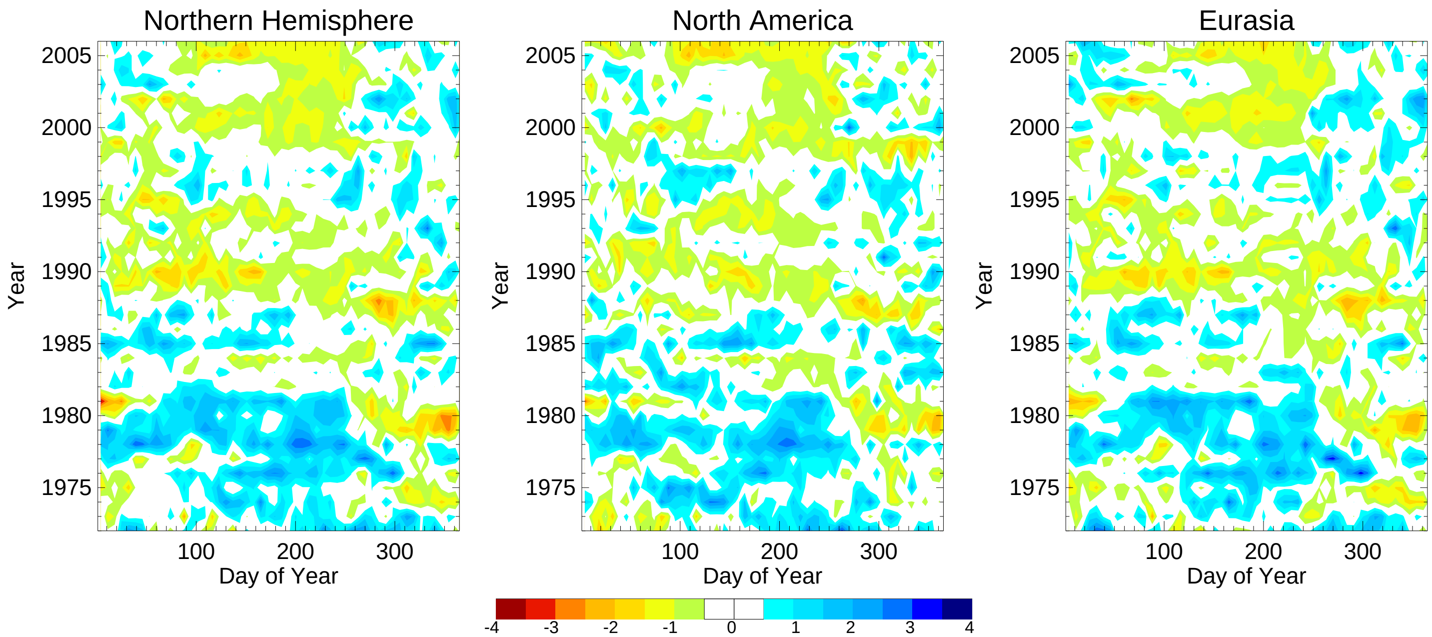
Northern Hemisphere
North America
Eurasia
Year
2005
2000
1995
1990
1985
1980
1975
100
200
300
Day of Year
-4
-3
-2
-1
0
1
2
3
4

Figure 3: